Control Engineering Practice 141 (2023) 105727

Contents lists available at ScienceDirect

Control Engineering Practice

journal homepage: www.elsevier.com/locate/conengprac

Human tracking from quantised sensors: An application to safe human–robot collaboration

Andrea Maria Zanchettin

Politecnico di Milano, Dipartimento di Elettronica, Informazione e Bioingegneria, Piazza Leonardo Da Vinci 32, Milano, Italy

ARTICLE INFO

Keywords:
Human–robot collaboration
Safety
Industrial robotics
Human detection and tracking

ABSTRACT

The proliferation of cage-less robotic applications is justifying this research which proposes a method to process the output of safety sensors with the aim of maximising the productivity of the robot in a collaborative scenario. Particularly, the Speed and Separation Monitoring (SSM) strategy, which prescribes the robot to reduce its speed proportionally to the vicinity of the human, will be investigated. In state-of-the-art industrial implementations, SSM is implemented in a very conservative way, without exploiting the capabilities of modern sensing devices. This work proposes a methodology to improve the performance of SSM algorithms while dealing finite and quantised 2D cost-effective sensing capabilities. The strategy is verified experimentally as applied on a palletising application with a Comau SmartSix industrial robot, showing slightly improved performance with respect to standard practice.

1. Introduction

Human detection and tracking is a longstanding research area with applications in human–robot collaboration (Bonci, Cen Cheng, Indri, Nabissi, & Sibona, 2021; Liu, Guo, Zou, & Duffy, 2022), and autonomous vehicles (Camara et al., 2020), among the others. One the most critical application of detection and tracking algorithms is for safety purposes (Robla-Gómez et al., 2017) which requires known (usually worst-case) uncertainty bounds, hard real-time capabilities, as well as compliance with relevant standards. Several technologies have been exploited for this purpose, ranging from ceiling mounted cameras (Bascetta et al., 2011), to vehicle mounted lidar sensors (Kidono, Miyasaka, Watanabe, Naito, & Miura, 2011).

Focusing on manufacturing applications, Kuhn et al. (Kuhn & Henrich, 2007) developed a camera-based system to estimate in real-time, directly within a single image frame, the distance between the worker and an industrial robot. A tactile floor mat has been proposed in Vogel, Fritzsche, and Elkmann (2016) to estimate the 2D position of the worker in the shop-floor. 3D Time of Flight (ToF) technologies have been exploited in several works (Kumar, Arora, & Sahin, 2019; Rosenstrauch & Krüger, 2018; Rosenstrauch, Pannen, & Krüger, 2018), while radar sensors have been adopted in Zlatanski, Sommer, Zurfluh, and Madonna (2018).

Beside the particular sensing technology, the problem of tracking humans and/or objects is of paramount importance, especially if some kind of model of the corresponding motion can be assumed to filter/correct noisy measurements.

Ibarguren, Maurtua, Pérez, and Sierra (2015) adopts a Particle Filter (PF) fed with measurements from a commercial laser rangefinder. In turn, Ragaglia, Zanchettin, and Rocco (2015) developed a Kalman Filter (KF) fed with a complete skeletal information of the worker whose output is then used to estimate the reachable set of the human within a prescribed prediction horizon. The work in Pereira and Althoff (2017) produces a similar output in a slightly different way.

From a robot control perspective, the Speed and Separation Monitoring (SSM) from ISO TC184/SC2 (2013) is the reference strategy to be considered in case of medium/large payload industrial robots, see Marvel and Norcross (2017) for an overview. In a nutshell, SSM prescribes to monitor the separating distance between the worker and the robot and to modulate the velocity of the manipulator in such a way that, at any time, the robot has enough deceleration capabilities to reduce its speed and stop before a possible contact occurs. A procedure, called risk-assessment, is then needed to tune and verify the parameters of the safety control strategy, Wadekar, Gopinath, and Johansen (2018). Several approaches are borrowed from SSM, as the works from Byner, Matthias, and Ding (2019) and Magrini et al. (2020), the one from Karagiannis et al. (2022), or the one from Lacevic, Zanchettin, and Rocco (2022) and Zanchettin and Lacevic (2022). They are mainly intended to derive speed reduction/modulation policies compliant with standards, while guaranteeing minimal intervention (i.e. high productivity). Other works, while still taking inspiration from SSM, are proposing dodging manoeuvres to prevent the robot from

E-mail address: andreamaria.zanchettin@polimi.it.

[1] An industrial-graded version is commercialised by Pilz as PSENmat with a spatial resolution of 1.0×0.6 m^2.

https://doi.org/10.1016/j.conengprac.2023.105727
Received 20 June 2023; Received in revised form 22 August 2023; Accepted 26 September 2023
Available online 9 October 2023

stopping or reducing its speed, Zanchettin, Rocco, Chiappa, and Rossi (2019).

Despite the proliferation of research works in the fields of sensing technologies and robot control strategies, industrial practice is substantially lagging in advancing the performance of commercial implementations of SSM. In fact, many of the methods available in the literature would be inapplicable in actual industrial settings as they require richer sensing information than those returned by commercial safety-rated devices. Commercial laser scanners, probably the mostly adopted sensing technology, can simultaneously monitor up to 64 areas (in the most recent 6-bits versions) where the human can be detected. In an average industrial work-cell of 36 m^2, this is translated in dividing the workspace in regular cells of 0.75 m of width. Similarly, the tactile floor mat described in Vogel et al. (2016)[1] has a width of 0.5 m. Independently from the specific sensing technology, the distance between the worker and the robot can be estimated up to that precision which might affect the performance of safety countermeasures.

This work introduces a methodology to improve the performance of SSM algorithms while assuming finite and quantised 2D sensing capabilities. The key idea stands in considering the velocity of the human as bounded from above, as also suggested in standards (ISO/TC 199, 2010). As a consequence, the distance between the robot workspace and the operator cannot instantaneously drop from one sensing cycle to the next one. It will be shown that the proposed strategy, fully compliant with safety standards, can outperform current practices with a reduced additional computational effort.

The reminder of this work is organised as follows. Section 2 introduces the method and its main properties. Section 3 describes the experimental facility and the experiments performed to validate the method. Finally, Section 4 discusses the main findings and the corresponding validation metrics, while Section 5 draws the conclusions.

2. Method

Speed and Separation Monitoring prescribes the robot to halt before any of its components can come into contact with the human operator. To achieve this goal, the workspace is monitored and the separation between the robot and the operator is measured. This safety functionality is implemented by defining velocity areas around the robot (see Fig. 1). Each velocity area is characterised by a maximum speed of the robot which is then actuated at lower level (TC 22/SC 22G, 2017), ranging from its nominal maximum speed, say 100% to a halting condition, 0%. State-of-the-art industrial practice simply relates the monitoring of the position of the human with one of these areas. In other words, safety sensors are demanded to check whether a certain area (see again Fig. 1) is occupied by the human or not. If so, the corresponding safety strategy is triggered.

Moving from this simplistic paradigm, we decouple the monitoring of the position of the operator from the corresponding action to be issued by the robot controller. In particular, as modern sensing techniques allow one to monitor more than a few areas, we will assume the workspace to be discretised at a finer level. The key idea will be to estimate the area occupied by the human operator in the workspace of the robot based on these discretised information. Then, the activation of the proper safety functionality can be implemented as in traditional applications.

Differently form other, yet similar, approaches in the literature relying on probability distributions, see e.g. Kim, Kirschner, Yamada, and Okamoto (2020), the method developed in this work assume a worst-case deterministic scenario of human movements, being better suited for industrial implementations.

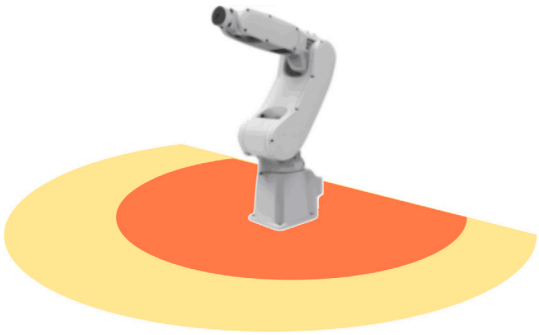

Fig. 1. Exemplification of the SSM functionality: when the yellow area is occupied a reduced speed is issued to the robot, while the presence of the operator in the red area forces the robot to stop completely. (For interpretation of the references to colour in this figure legend, the reader is referred to the web version of this article.)

2.1. Generalities

Assume that the position of the worker at discrete time $k-1$, say $\boldsymbol{x}_{k-1|k-1} \in \mathbb{R}^2$, is available in terms of a probability distribution $\mathcal{D}$ defined over the support $\mathcal{H}_{k-1|k-1}$ (which is assumed to be a limited compact set in $\mathbb{R}^2$), i.e. $\boldsymbol{x}_{k-1|k-1} \sim \mathcal{D}\left(\mathcal{H}_{k-1|k-1}\right)$. Notice that, from a safety perspective, the actual shape of $\mathcal{D}$ is not a relevant information. Therefore, we only focus on the estimation of the support (i.e. the region of the working space with non-null probability to be occupied). The goal of this work is then to update the support of such a distribution to be later used as a safety-rated measurement. We assume the walking velocity of the worker to be limited from above, as suggested in safety standards (ISO/TC 199, 2010), by $v^{\max} > 0$. Then, given $\mathcal{H}_{k-1|k-1}$ from the previous cycle, one can predict the support of the distribution of $\boldsymbol{x}_{k|k-1}$ as follows

$$\mathcal{H}_{k|k-1} = \mathcal{H}_{k-1|k-1} \oplus \mathcal{B}\left(v^{\max} T_s\right) \tag{1}$$

where $\oplus$ represents the Minkowski sum,[2] T_s is the sampling time, while $\mathcal{B}(\rho)$ stands for a generic $\mathbb{R}^2$-ball of radius $\rho > 0$ centred in the origin, i.e. $\mathcal{B}(\rho) = \left\{\boldsymbol{x} \in \mathbb{R}^2 : \|\boldsymbol{x}\| \leq \rho\right\}$. The set $\mathcal{B}(\rho)$ represents the reachable set from the origin of the human, assuming his/her walking speed is not exceeding $v^{\max}$, the Minkowski sum $\oplus$ is used to apply the reachable set to $\mathcal{H}_{k-1|k-1}$, rather than to the origin. Overall, set $\mathcal{H}_{k|k-1}$ constitutes the reachable set from $\mathcal{H}_{k-1|k-1}$ in one discrete time instant, and represents only a model-based *prediction* of the support of the distribution of the position of the worker at the current time instant, i.e. $\boldsymbol{x}_{k|k-1} \sim \mathcal{D}\left(\mathcal{H}_{k|k-1}\right)$.

Assume the workspace around the robot to be monitored by one or more safety sensors, each responsible for a specific area $\mathcal{Z}_i \subset \mathbb{R}^2, i = 1, \ldots, n$, where $i \neq j : \mathcal{Z}_i \cap \mathcal{Z}_j = \emptyset$ (areas are not overlapping each other). Further assume that $b_{ik} \in \{0, 1\}$ indicates whether or not the human has been detected in area i at discrete time instant k. Then, the *update* phase can be handled intersecting the information coming from measurements with the set $\mathcal{H}_{k|k-1}$ obtained in the prediction phase, i.e.

$$\mathcal{H}_{k|k} = \mathcal{H}_{k|k-1} \cap \bigcup_{i=1}^{n} \begin{cases} \mathcal{Z}_i & b_{ik} = 1 \\ \emptyset & \text{otherwise} \end{cases} \tag{2}$$

which represents the best estimate of the support of the distribution of the position of the worker at current time instant, i.e. $\boldsymbol{x}_{k|k} \sim \mathcal{D}\left(\mathcal{H}_{k|k}\right)$.

The two phases (1) and (2) (i.e. prediction and update) are exemplified in Fig. 2 and represent the closed-form Bayesian recursive estimation (Bayesian Filter) of the support of the continuous distribution representing the position of the worker in the shop-floor.

[1] An industrial-graded version is commercialised by Pilz as PSENmat with a spatial resolution of 1.0×0.6 m^2.

[2] Given two sets $\mathcal{A}$ and $\mathcal{B}$, their Minkowski sum $\mathcal{C} = \mathcal{A} \oplus \mathcal{B}$ is the set $\mathcal{C} = \{x + y, x \in \mathcal{A}, y \in \mathcal{B}\}$.

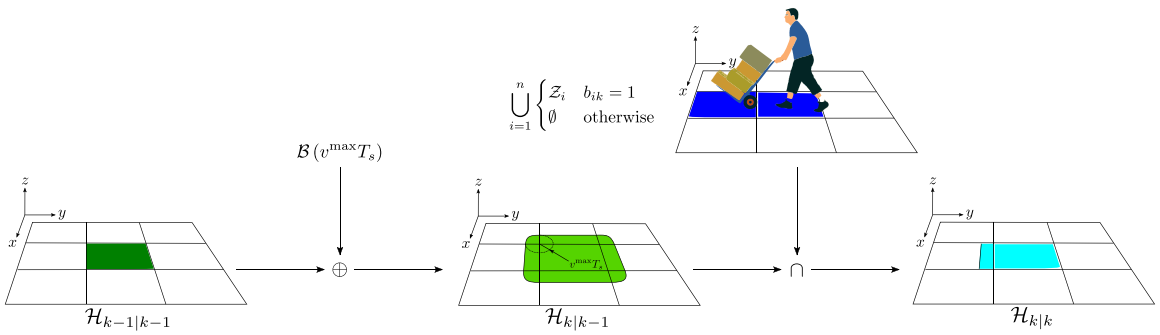

Fig. 2. Exemplification of the prediction/update procedure in (2): area occupied by the human at time instant $k-1$ ($\mathcal{H}_{k-1|k-1}$, left), prediction of the area occupied at time $k-1$ based on reachable set ($\mathcal{H}_{k|k-1}$, centre), and area occupied at k ($\mathcal{H}_{k|k}$, right), consistent with sensor readings (top).

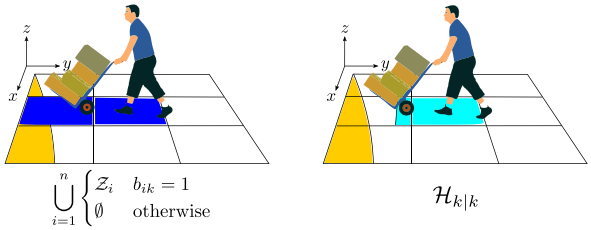

Fig. 3. Area on the ground occupied by the worker using sensor measurements only (left) and the method in (2) (right) with respect to a safety area (orange) centred around the robot. In the first case (on the left) the safety functionality will be triggered, in the latter (right) it will not. (For interpretation of the references to colour in this figure legend, the reader is referred to the web version of this article.)

Remark 1. From (2), it follows immediately that

$$\mathcal{H}_{k|k} \subseteq \bigcup_{i=1}^{n} \begin{cases} \mathcal{Z}_i & b_{ik} = 1 \\ \emptyset & \text{otherwise} \end{cases}$$

This property, which simply indicates that the sensor readings are likely to produce an overestimation of the support of the distribution of positions possibly occupied by the worker, is extremely important when it comes for the robot controller to decide to trigger or not a safety functionality. As an example, consider a circular safety zone around the robot which triggers a safety limited speed (SLS, TC 22/SC 22G, 2017) functionality. Its radius depends mainly on risk assessment parameters and can be computed using the stopping time and the reach of the robot, $v^{\max}$, as well as the intrusion distance C, i.e. the length of a part of the body within the safety zone and towards the robot, prior to actuation of the safeguard, ISO/TC 199 (2010). The safety functionality is trigger as soon as a foot of the worker is detected inside. It is then clear that a better estimation of the area on the ground occupied by the worker would reduce the activation of the safety functionalities, yielding to a more productive application (see Fig. 3).

2.2. Initialisation, the case of $\mathcal{H}_{k-1|k-1} = \emptyset$

Eq. (2) allows one to track the area occupied by the human and hence requires the quantity $\mathcal{H}_{k-1|k-1}$ to be available from previous computations. If this is not the case, i.e. at the startup of the application, or in general when $\mathcal{H}_{k-1|k-1} = \emptyset$, Eq. (2) is not applicable (it would yield to $\mathcal{H}_{k|k} = \emptyset$ not matter the value of b_{ik}).

For this reason, an ad hoc procedure handling the detection phase has to be developed. The simplest way to handle the startup phase is to initialise $\mathcal{H}_{k|k}$ as follows

$$\mathcal{H}_{k|k} = \bigcup_{i=1}^{n} \begin{cases} \mathcal{Z}_i & b_{ik} = 1 \\ \emptyset & \text{otherwise} \end{cases} \tag{3}$$

The initialisation formula (3) can be used both at the startup of the application as well as whenever $\mathcal{H}_{k-1|k-1} = \emptyset$. In both the two cases, in fact, no previous measurement is available. It should be noticed that this situation might happen also during the operation phase, when no human is detected at time instant $k-1$. Algorithm 1 sketches the main phases of the algorithm.

Algorithm 1 Tracking of human position in the workspace

```
if H_{k-1|k-1} = ∅ then
    // initialisation
    H_{k|k} ← ∅;
    for i = 1, ..., n do
        if b_{ik} = 1 then
            H_{k|k} ← H_{k|k} ∪ Z_i;
else
    // prediction
    H_{k|k-1} ← H_{k-1|k-1} ⊕ B(v^max T_s);
    T ← ∅;
    for i = 1, ..., n do
        if b_{ik} = 1 then
            T ← T ∪ Z_i;
    // update
    H_{k|k} ← H_{k|k-1} ∩ T;
k ← k + 1;
```

3. Validation experiments

An experimental validation campaign has been organised involving $N = 11$ volunteers (aged from 24 to 56). The experiments are run in a mockup palletisation facility (see Fig. 4). A collaborative palletisation has been selected as representative of all applications requiring a sporadic interaction between the worker and the robot in which safety can be efficiently handled via SSM. Applications requiring more frequent interactions, like, e.g., assembly, are better handled with other safety strategies like Power and Force Limiting (PFL, see again ISO TC184/SC2, 2013).

Three velocity levels have been designed: 100% (with a speed of the tool centre point up to 1.5 ms^{-1}), 10%, and 0%. The radii of the corresponding two areas (see the yellow and the red ones in Fig. 1) have been computed as

$$\rho_\alpha = v^{\max} T_{b,\alpha} + C + R$$

where $v^{\max} = 1.6$ ms^{-1} (ISO/TC 199, 2010), $C = 0.7$ m stands for the intrusion distance (i.e. the distance that a part of the body, typically the arms, can intrude into the velocity area before the intrusion is actually detected), $R = 1.2$ m represents the reach of the robot within the selected application, α has been set equal to either 1.0 (for the yellow) or 0.1 (for the red area), while $T_{b,\alpha}$ is the corresponding robot braking time. Specifically, the following parameters have been considered:

$$\rho_{1.0} = 3.0, \quad \rho_{0.1} = 2.0$$

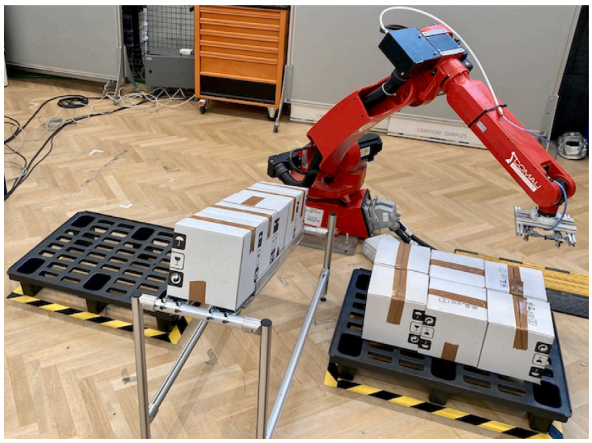

Fig. 4. Setup for the experimental verification: a Comau SmartSix industrial robot adopted in a palletising application and a sensor (not visible in the picture) which returns the active areas b_{ik}'s.

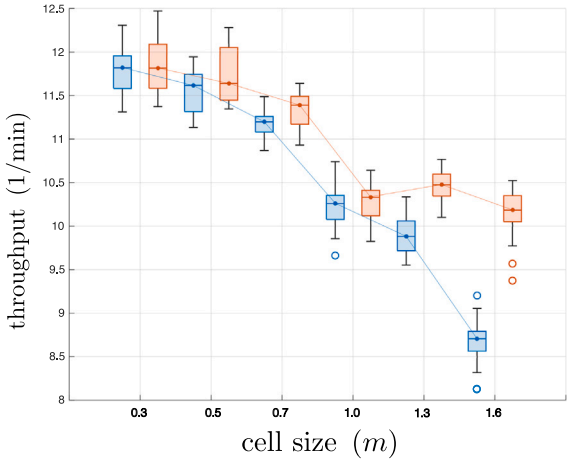

Fig. 5. Distribution of throughput (palletisation cycles per minute) depending on the quantisation of the cell, with (red) and without (blue) the prediction method proposed in this paper. (For interpretation of the references to colour in this figure legend, the reader is referred to the web version of this article.)

Two robot safety policies have been implemented: (1) the former only relies on the distance computed based on occupied areas $\mathcal{Z}_i$ (i.e. running an excerpt of Algorithm 1 composed by lines 2–6, only) and will be considered as baseline as it corresponds to the current practice, while (2) the latter is based on $\mathcal{H}_{k|k}$ which is updated based on a full execution of Algorithm 1 which is also summarised in the block diagram of Fig. 7. In order to address the sensitivity of the performance of the proposed method with respect to the dimensions of the zones, several simulations have been performed, varying the dimension of the size of each square zone $\mathcal{Z}_i$, ranging from 0.3 to 1.6 m.

The position of the human has been generated according to the following trajectory

$$x(t) = A_x \sin\left(\alpha\omega_x t + \frac{\pi}{2}\right), y(t) = 3 + A_y \sin\left(\alpha\omega_y t\right)$$

where $A_x = 3, A_y = 2, \omega_x = 1, \omega_y = 2$. The parameter α has been defined as

$$\alpha = \frac{v}{\sqrt{A_x^2\omega_x^2 + A_y^2\omega_y^2}}$$

so that $\sqrt{\dot{x}^2(t) + \dot{y}^2(t)} \leq v$, while v is extracted randomly, in each simulation, from a uniform distribution from 1.0 to $v^{\max} = 1.6$ ms^{-1}.

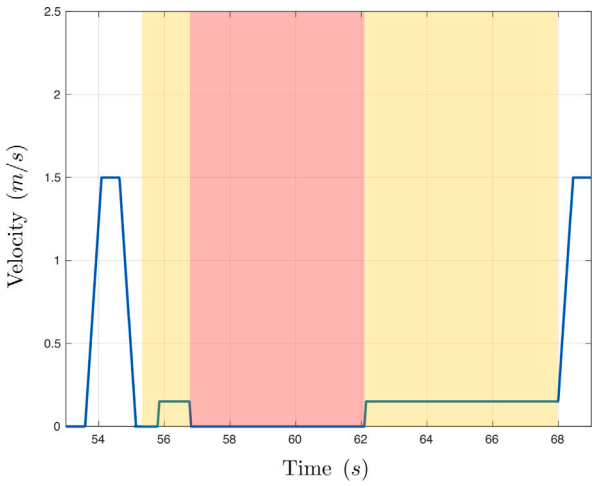

Fig. 6. Velocity of the robot along the path depending on the active velocity level which is evaluated based on the intersection between $\mathcal{H}_{k|k}$ and the velocity areas see again Fig. 1. The velocity of the robot along its path is reduced either to 10% of the nominal value, i.e. to 0.15 ms^{-1}, when the yellow area is active, or to 10% in case of activation of the red area. (For interpretation of the references to colour in this figure legend, the reader is referred to the web version of this article.)

For each configuration, 40 runs have been performed, collecting data from a total number of 240 simulations. Fig. 5 reports the throughput of the palletising application (in terms of boxes per minute) depending on the dimension of the areas $\mathcal{Z}_i$. The throughput seems to be negatively correlated with the dimensions of the zone, thought its behaviour does not present any linear trend. Interestingly, a substantial drop in the performance of the application when the size of the cells are reduced from 0.5 m to 1.0 m. If compared with a baseline method with no prediction, the drop in the performance of the application is less evident when the prediction algorithm proposed in this paper is adopted.

In the view of the discussion above, within the experimental verification, two different settings for the discretisation of the environment to be monitored have been considered: (A) a fine-grained quantisation with cells $\mathcal{Z}_i$ of size 0.5×0.5 m, and (B) a coarse one, with dimensions 1.0×1.0 m.

Certainly, adaptive velocity areas tailored around the actual robot position, as proposed in Karagiannis et al. (2022), would certainly improve the performance. On the other hand, since the main focus of this work is on the tracking problem of the human in the working area of the robot, we will stick to the traditional approach of fixed areas, as the ones in Fig. 1, which is more aligned with state-of-the-art industrial implementations. Fig. 6 reports an example of the behaviour of the safety algorithm implemented in the robot controller.

Each of the N volunteers interact with the robot in all the four possible cases (i.e. A1, A2, B1, and B2, as specified above), in that or reversed order. In order to obtain comparable results, volunteers are instructed to walk on specific paths (marked on the floor) around and towards the robot (see again Fig. 4) for the whole duration of the experiment and to count to two whenever a marked position is reached. No other instructions were given to the volunteers. Per each experiment (four per each of the N volunteers), the following Key Performance Indicators (KPIs) have been extracted:

- the average throughput in terms of palletising cycles (picking from the gravity flow rack and placing onto the pallet) per minute;
- the average area representing the human in the collaborative workspace.

The former is intended for the comparison of the productivity of the collaborative application depending on the particular setting (fine vs.

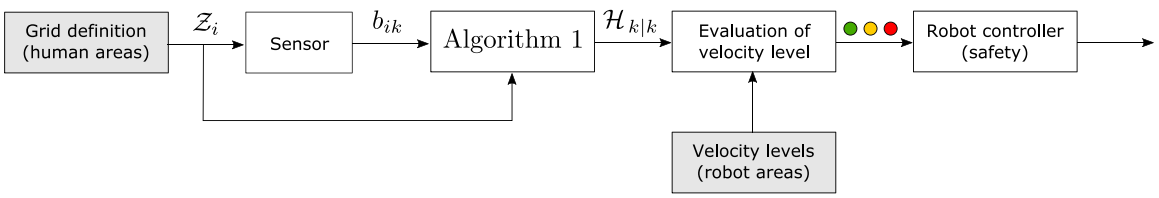

Fig. 7. Block diagram of the proposed methodology (grey boxes are offline functionalities for the setup of the application and of the corresponding parameters which are typically set during the risk assessment, Chemweno, Pintelon, & Decre, 2020).

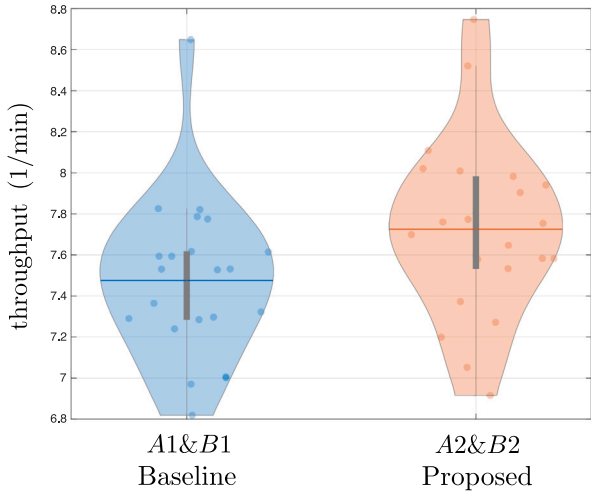

Fig. 8. Inter-subject analysis of the increased productivity ascribable to the proposed algorithm ($A2\&B2$, right) with respect to the baseline ($A1\&B1$, left).

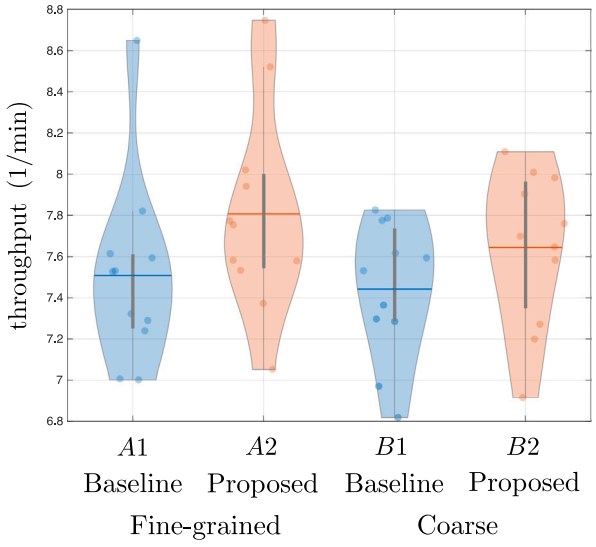

Fig. 9. Inter-subject analysis of the throughput (palletisation cycles per minute) depending on the particular setting.

grained quantisation, and with and without the proposed algorithm). In turn, the latter is intended to be used for an empirical verification of Remark 1.

4. Findings and discussion

The analysis of the collected data has been divided into two distinct parts: an inter-subject analysis and an intra-subject one. The inter-subject is intended to address the overall performance of the method as applied in its different settings. In turn, the intra-subject analysis is intended to better understand whether the outcome of the inter-subject analysis can be extended to all the subjects, at least with sufficient statistical significance.

4.1. Inter-subject analysis

The first analyses are focused on the average throughput of the application, in terms of cycles per minute. Fig. 8 reports the distribution of the throughput as a function of the applied method. The method developed in this work ($A2\&B2$) is responsible for an increased productivity ($p = 0.02$, Wilcoxon) from 449 to 464 items per hour (+3.34%) on average.

In order to better understand the effects of the workspace quantisation, if any, Fig. 9 reports the throughput of the collaborative application in the four different settings, i.e. A1 (fine-grained quantisation without the developed algorithm), A2 (fine-grained quantisation with the developed algorithm), B1 and B2 (coarse quantisation without and with the developed algorithm, respectively).

For the fine-grained quantisation (A), the adoption of Algorithm 1 contributes in increasing the productivity with respect to the baseline ($p = 0.04$, Wilcoxon), from approximately 451 to 468 items per hour (+4.0%). Similar results can be qualitatively observed for the coarse quantisation (B), though without statistical significance ($p = 0.12$, Wilcoxon), from 447 to 459 items per hour (+2.7%).

As per the empirical verification of Remark 1, the size of the areas representing the occupation of the human are reported in Fig. 10 in the four possible settings. With a high statistical significance, the area representing the human occupancy in the workspace is always lower when Algorithm 1 is adopted ($p = 4.1 \cdot 10^{-5}$, Wilcoxon), regardless the quantisation. This outcome was indeed expected as a direct consequence of Remark 1, which is indeed formally stating the empirical finding.

4.2. Intra-subject analysis

In the following, the outcome of the intra-subject analysis is reported. As already mentioned, the intra-subject analysis is intended to verify whether the findings regarding the increased throughput can be extended to each specific subject. Fig. 11 reports the distribution of the difference in the average throughputs obtained with and without the proposed methodology for the two different quantisations. For almost all the subjects, the adoption of prediction/update method in Algorithm 1 is capable of increasing the productivity of the palletising application in terms of a +4.0% speed-up in the case of a fine-grained quantisation ($p < 0.01$, Student). The same has been found, though with a smaller significance, for the coarse-grained case ($p = 0.02$, Student), with an average speed-up of +2.8%. Finally, though it might seem from Fig. 11 that a finer quantisation is capable of increasing the throughput more with respect to a more coarse one, this fact has no statistical significance ($p = 0.22$, Student), at least in the collected data.

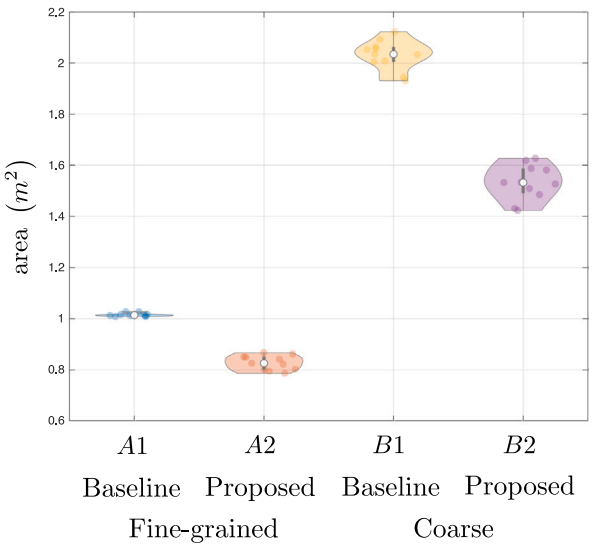

Fig. 10. Inter-subject analysis of the average area occupied by the human depending on the particular setting.

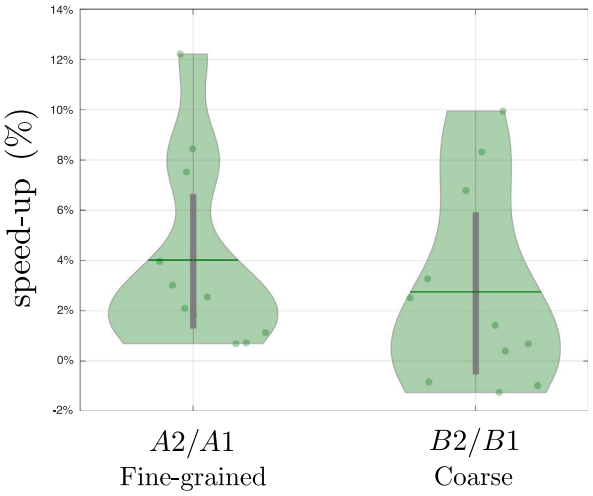

Fig. 11. Intra-subject analysis of the increased productivity ascribable to the proposed algorithm in the two quantisation settings (fine, A, on the left, and coarse, B, on the right).

4.3. Discussion

The experimental campaign has demonstrated the possibility to slightly increase the throughput, at least in the given application, by adopting the proposed methodology. The benefit in terms of productivity seems to be more likely to happen for a fine quantisation. From an intra-subject perspective, the increased throughput is guaranteed, with rare exceptions. Though the speed-up in the application seems to be marginal (+4.0% for the fine-grained quantisation, +2.8% for the coarse one), in the long run, the methodology developed in this paper can bring a substantial benefit to the efficiency of a cage-free robotic installation. This finding allows us to draw some conclusions regarding further possible research developments in the field of sensing technologies and related signal processing. From the one hand, a better handling of quantised measurement, for example adopting the method proposed in this work, might in principle increase the performance of a collaborative robotic application that does not require a persistent interaction between the robot and the human operator. Additionally, higher resolutions do not seem to substantially increase the performance of the safety system. From the other hand, we believe that a better and less conservative safety strategy implemented within the robot controller (see, e.g., Karagiannis et al., 2022; Zanchettin & Lacevic, 2022 for a few examples) would be way more effective in increasing the productivity. The reason why the most simplistic, yet conservative, approach (see once again Fig. 1) has been selected for the experimental verification has to be found in the industrial best practice.

In addition, from the sensitivity analysis reported in Fig. 5, it is evident that a substantial reduction of the quantisation (e.g. from 0.7 to 0.3 m in size) does not contribute in a comparable increase of the throughput. This is mainly due to the enlarged occupancy of the human during the prediction phase. Within the proposed method such an enlarged occupancy grows with a rate of $v^{\max}T_s$, instead of being considered as a lumped value of $v^{\max}T_{b,a}$. A less conservative value of $v^{\max}$ or the inclusion of a more accurate kinematic model of the human motion, as proposed in Ragaglia et al. (2015), would positively affect the performance. Moreover, the adoption of a 3D sensor, rather than a floor-level sensing technology, will also pave the way for a less conservative approach to safety. On the other hand, no guidelines on how to handle the prediction of human upper limbs are given in the most recent versions of safety standards.

5. Conclusions

This work proposed a method to estimate the area occupied by the human operator on the shop-floor of a collaborative robotic application, while dealing finite and quantised 2D sensing capabilities. A sensitivity analysis has shown that a finer quantisation does not necessarily correspond to increased performances. The strategy has been verified experimentally in a collaborative palletising application. The method, as applied to the given application, has shown a general increase in terms of productivity of the application. Further research can be focused on extending the method to work with 3D sensing technologies. On the other hand, an additional effort from standardisation committees will be required to provide guidelines on how to consider the occupancy of human upper limbs.

Declaration of competing interest

The author declares no particular interest.

Acknowledgements

This study was partially carried out within the MICS (Made in Italy – Circular and Sustainable) Extended Partnership and received funding from Next-Generation EU (Italian PNRR – M4 C2, Invest 1.3 – D.D. 1551.11-10-2022, PE00000004). CUP MICS D43C22003120001.

References

Bascetta, L., Ferretti, G., Rocco, P., Ardö, H., Bruyninckx, H., Demeester, E., et al. (2011). Towards safe human-robot interaction in robotic cells: an approach based on visual tracking and intention estimation. In *2011 IEEE/RSJ international conference on intelligent robots and systems* (pp. 2971–2978). IEEE.

Bonci, A., Cen Cheng, P. D., Indri, M., Nabissi, G., & Sibona, F. (2021). Human-robot perception in industrial environments: A survey. *Sensors*, *21*(5), 1571.

Byner, C., Matthias, B., & Ding, H. (2019). Dynamic speed and separation monitoring for collaborative robot applications–concepts and performance. *Robotics and Computer-Integrated Manufacturing*, *58*, 239–252.

Camara, F., Bellotto, N., Cosar, S., Nathanael, D., Althoff, M., Wu, J., et al. (2020). Pedestrian models for autonomous driving part I: Low-level models, from sensing to tracking. *IEEE Transactions on Intelligent Transportation Systems*, *22*(10), 6131–6151.

Chemweno, P., Pintelon, L., & Decre, W. (2020). Orienting safety assurance with outcomes of hazard analysis and risk assessment: A review of the ISO 15066 standard for collaborative robot systems. *Safety Science*, *129*, Article 104832.

Ibarguren, A., Maurtua, I., Pérez, M. A., & Sierra, B. (2015). Multiple target tracking based on particle filtering for safety in industrial robotic cells. *Robotics and Autonomous Systems*, *72*, 105–113.

ISO TC184/SC2 (2013). ISO/TS 15066 robots and robotic devices – Safety requirements for industrial robots – collaborative operation.

ISO/TC 199 (2010). ISO 13855:2010 - safety of machinery - positioning of safeguards with respect to the approach speeds of parts of the human body.

Karagiannis, P., Kousi, N., Michalos, G., Dimoulas, K., Mparis, K., Dimosthenopoulos, D., et al. (2022). Adaptive speed and separation monitoring based on switching of safety zones for effective human robot collaboration. *Robotics and Computer-Integrated Manufacturing*, *77*, Article 102361.

Kidono, K., Miyasaka, T., Watanabe, A., Naito, T., & Miura, J. (2011). Pedestrian recognition using high-definition LIDAR. In *2011 IEEE intelligent vehicles symposium* (pp. 405–410). IEEE.

Kim, E., Kirschner, R., Yamada, Y., & Okamoto, S. (2020). Estimating probability of human hand intrusion for speed and separation monitoring using interference theory. *Robotics and Computer-Integrated Manufacturing*, *61*, Article 101819.

Kuhn, S., & Henrich, D. (2007). Fast vision-based minimum distance determination between known and unkown objects. In *2007 IEEE/RSJ international conference on intelligent robots and systems* (pp. 2186–2191). IEEE.

Kumar, S., Arora, S., & Sahin, F. (2019). Speed and separation monitoring using on-robot time-of-flight laser-ranging sensor arrays. In *2019 IEEE 15th international conference on automation science and engineering* (pp. 1684–1691). IEEE.

Lacevic, B., Zanchettin, A. M., & Rocco, P. (2022). Safe human-robot collaboration via collision checking and explicit representation of danger zones. *IEEE Transactions on Automation Science and Engineering*, 1–16.

Liu, L., Guo, F., Zou, Z., & Duffy, V. G. (2022). Application, development and future opportunities of collaborative robots (cobots) in manufacturing: A literature review. *International Journal of Human–Computer Interaction*, 1–18.

Magrini, E., Ferraguti, F., Ronga, A. J., Pini, F., De Luca, A., & Leali, F. (2020). Human-robot coexistence and interaction in open industrial cells. *Robotics and Computer-Integrated Manufacturing*, *61*, Article 101846.

Marvel, J. A., & Norcross, R. (2017). Implementing speed and separation monitoring in collaborative robot workcells. *Robotics and Computer-Integrated Manufacturing*, *44*, 144–155.

Pereira, A., & Althoff, M. (2017). Overapproximative human arm occupancy prediction for collision avoidance. *IEEE Transactions on Automation Science and Engineering*, *15*(2), 818–831.

Ragaglia, M., Zanchettin, A. M., & Rocco, P. (2015). Safety-aware trajectory scaling for human-robot collaboration with prediction of human occupancy. In *2015 International conference on advanced robotics* (pp. 85–90). IEEE.

Robla-Gómez, S., Becerra, V. M., Llata, J. R., Gonzalez-Sarabia, E., Torre-Ferrero, C., & Perez-Oria, J. (2017). Working together: A review on safe human-robot collaboration in industrial environments. *IEEE Access*, *5*, 26754–26773.

Rosenstrauch, M. J., & Krüger, J. (2018). Safe human robot collaboration operation area segmentation for dynamic adjustable distance monitoring. In *2018 4th International conference on control, automation and robotics* (pp. 17–21). IEEE.

Rosenstrauch, M. J., Pannen, T. J., & Krüger, J. (2018). Human robot collaboration-using kinect v2 for ISO/TS 15066 speed and separation monitoring. *Procedia CIRP*, *76*, 183–186.

TC 22/SC 22G (2017). IEC adjustable speed electrical power drive systems safety requirements. Functional.

Vogel, C., Fritzsche, M., & Elkmann, N. (2016). Safe human-robot cooperation with high-payload robots in industrial applications. In *2016 11th ACM/IEEE international conference on human-robot interaction* (pp. 529–530). IEEE.

Wadekar, P., Gopinath, V., & Johansen, K. (2018). Safe layout design and evaluation of a human-robot collaborative application cell through risk assessment–A computer aided approach. *Procedia Manufacturing*, *25*, 602–611.

Zanchettin, A. M., & Lacevic, B. (2022). Safe and minimum-time path-following problem for collaborative industrial robots. *Journal of Manufacturing Systems*, *65*, 686–693.

Zanchettin, A. M., Rocco, P., Chiappa, S., & Rossi, R. (2019). Towards an optimal avoidance strategy for collaborative robots. *Robotics and Computer-Integrated Manufacturing*, *59*, 47–55.

Zlatanski, M., Sommer, P., Zurfluh, F., & Madonna, G. L. (2018). Radar sensor for fenceless machine guarding and collaborative robotics. In *2018 IEEE international conference on intelligence and safety for robotics* (pp. 19–25). IEEE.